Icarus xxx (xxxx) xxx–xxx

Contents lists available at ScienceDirect

Icarus

journal homepage: www.elsevier.com/locate/icarus

Titan's ionospheric chemistry, fullerenes, oxygen, galactic cosmic rays and the formation of exobiological molecules on and within its surfaces and lakes

Edward C. Sittler Jr[a,*], John F. Cooper[b], Steven J. Sturner[c,d], Ashraf Ali[e,f]

[a] *Geospace Physics Laboratory, Code 673, NASA Goddard Space Flight Center, Greenbelt, MD 20771, United States of America*
[b] *Heliospheric Physics Laboratory, Code 672, NASA Goddard Space Flight Center, Greenbelt, MD 20771, United States of America*
[c] *University of Maryland, Baltimore County, Goddard Planetary Heliophysics Institute, Baltimore, MD 21250, United States of America*
[d] *Code 661, NASA Goddard Space Flight Center, Greenbelt, MD 20771, United States of America*
[e] *SSAI, Greenbelt, MD, United States of America*
[f] *University of Maryland College Park, MD, 20740, United States of America*

ABSTRACT

We discuss the formation of aerosols within Titan's thermosphere-ionosphere and the different chemical pathways. Negative ion measurements by the Cassini Plasma Spectrometer (CAPS) Electron Spectrometer (ELS) give evidence for formation of unsaturated anion carbon chains, while positive ion measurements of the Cassini Ion Neutral Mass Spectrometer (INMS) indicate formation of more aromatic cation hydrocarbons. There is presently no direct observational evidence for large neutral molecule growth in Titan's thermosphere-ionosphere. The hydrocarbon cations are expected to form Polycyclic Aromatic Hydrocarbons (PAH), those with the addition of nitrogen being called PAHNs. We theorize anion carbon chains can eventually become long enough to fold into fullerene $C_{60,70}$ carbon shells, of various charge states. Based on laboratory data the fullerenes can trap incoming O^+ magnetospheric ions that have relatively high energy collisions with the fullerenes and, once trapped, protect the oxygen atom from Titan's reducing thermosphere-ionosphere. The fullerenes can form into larger onion fullerenes and condense into larger embryo aerosols (i.e., $m/q > 10{,}000$ amu/q anions as observed by CAPS/ELS) eventually falling onto Titan's surface and precipitating to the bottom of its hydrocarbon lakes. Molecule production composed of H, C, N is known to occur in Titan's atmosphere with energy input from the magnetosphere, solar UV, and deep-penetrating irradiation from galactic cosmic rays (GCR). Space radiation effects by GCR irradiation of Titan's surface and lakes can lead to the manufacture of exobiological molecules with oxygen as the new ingredient. We have developed a model of galactic cosmic ray irradiation of Titan's atmosphere, surface, subsurface and bottoms of Titan lakes. GCR would provide further energy for processing of the aerosols into more complex organic forms such as tholins and precursor molecules for amino acids. A second process called hydrolysis then converts the precursor molecules into amino acids. Hydrolysis is provided via meteor impacts with size > 10 km and cryovolcanism both which can produce liquid water on Titan's surface for episodic periods > several 100 to 1000 years. Our model shows that GCR secondary particles can penetrate ~ 100 m below the ice surface (including the bottom of Titan's less dense hydrocarbon lakes ~ 150 m depths) and produce chemically significant dosages over very long timescales ~ 450 Myrs. The GCR model is combined with laboratory data from experiments in which dry methyl ices were irradiated to doses producing prebiotic amino acids such as glycine. The model calculations show glycine can form to ~ 2.5 ppb levels near the surface after ~ 450 Myrs of GCR proton irradiation and potentially to 5 ppb if heavy-ion GCRs up through Fe are included. If such molecules were detected, this would not only confirm this model but indicate that life forms different from ours may not be required.

1. Introduction

We have advanced the development of a model first presented by Sittler Jr. et al. (2009a) on the formation of fullerenes within Titan's ionosphere based on the discovery of heavy anions within Titan's ionosphere by Coates et al. (2007) who used Cassini Plasma Spectrometer (CAPS) Electron Spectrometer (ELS) observations. Based on analogies of anion carbon chains observed to be forming within molecular clouds and planetary nebula (Cami et al., 2010; Bernard-Salas et al., 2012; Ehrenfreund and Foing, 2010) and their thermodynamic similarities with Titan, we argued for anion carbon chain formation within Titan's ionosphere-thermosphere. Once long enough, these chains will fold into (Kroto et al., 1985; Kroto et al., 1991) spherical shells of carbon atoms C_{60} or ellipsoidal shells of carbon atoms C_{70} called fullerenes as determined by Krätschmer et al. (1990) using x-ray crystallography techniques. These fullerenes would tend to form below the ionospheric peak down near 950 km where the largest anions were discovered by Coates et al. (2007). In the earlier paper we then argued that keV O^+

---

[*] Corresponding author.
E-mail addresses: edward.c.sittler@nasa.gov (E.C. Sittler), john.f.cooper@nasa.gov (J.F. Cooper), steven.j.sturner@nasa.gov (S.J. Sturner), aali1234@umd.edu (A. Ali).

https://doi.org/10.1016/j.icarus.2019.03.023
Received 4 April 2018; Received in revised form 8 March 2019; Accepted 13 March 2019

Please cite this article as: Edward C. Sittler, et al., Icarus, https://doi.org/10.1016/j.icarus.2019.03.023

ions from Saturn's magnetosphere could become trapped within the fullerenes based on lab measurements of noble gases such as ^{4}He (Weiske et al., 1991), ^{40}Ar (Caldwell et al., 1992) and nitrogen atoms (Pietzak et al., 1997; Weidinger et al., 1998) being trapped within the fullerenes from high energy collisions ~ 100 eV per incident atom. The model of Cravens et al. (2008) defined the penetration of magnetosphere keV oxygen ions within Titan's ionosphere down to altitudes < 950 km, where we find that the oxygen atoms could become trapped within the fullerenes. Within the fullerenes the oxygen atoms are isolated from Titan's reducing atmosphere as the fullerenes condense into larger aerosols and eventually precipitate onto Titan's surface and hydrocarbon lakes. This model has been given more credence due to the recent analysis of the CAPS ELS observations of anions by Desai et al. (2017) who showed the presence of anion carbon chains within Titan's ionosphere. In the present paper is a model of the interactions of Galactic Cosmic Rays (GCR) including the transport of GCR primary proton and secondary interaction components through the atmosphere to the surface and 100's of meters depth into the sub-surface. This model, which is similar to that developed by others (i.e., Molina-Cuberos et al., 1999; Borucki et al., 2006 which were more focused on the ionization of Titan's dense lower atmosphere), allows us to explore the possibility of exobiological formation within Titan's subsurface and lakebeds where the precipitated aerosols would accumulate.

Hudson et al. (2008) produced significant abundances of amino acids such as glycine using a two-step process from MeV proton irradiation of dry acetonitrile (CH_3CN) ice at dosage levels ~ 60 Gigarad (6×10^8 Grays) to produce solid residues composed of molecular precursors that, after acid hydrolysis, yielded amino acids such as glycine, the building blocks of life as we know it. They estimated water contamination < 0.001% for the CH_3CN sample without H_2O, and use acid hydrolysis (which they note is equivalent with water hydrolysis occurring over long periods of time with the acid acting as a catalyst) for amino acid presence in their samples. In the case of Titan, we propose the hydrolysis of the precursor molecules is provided by meteor impacts > 10 km in size and cryovolcanism to produce liquid water on the surface and interact with the tholins on the surface that have already been processed by the GCR (Lunine, 1990; Sagan et al., 1992; Thompson and Sagan, 1992; Artemieva and Lunine, 2003). If our model is confirmed by future observations, the oxygen problem is solved by providing the missing oxygen trapped within the fullerenes that feed into the aerosols and eventually the tholins on Titan's surface and subsurface. From these irradiation data one can estimate the abundances of various exobiological molecules within Titan surfaces and lakes as functions of irradiation rates from GCRs. Here, we note three discoveries that allowed such chemistry to occur at Titan: 1) Enceladus injection of large amounts ~ 10^{28} mol/s of water vapor into Saturn's magnetosphere (Porco et al., 2006; Hansen et al., 2006; Burger et al., 2007; Sittler Jr. et al., 2008; Waite et al., 2009a), 2) keV oxygen ions from Saturn's magnetosphere (average integral flux ~ $4 \times 10^5\ O^+/cm^2$-s of oxygen ions or globally ~ 5.6×10^{23} ions/s) to enter Titan's thermosphere-ionosphere (Hartle et al., 2006a, 2006b), and 3) large positive (Waite Jr. et al., 2007; Crary et al., 2009; Waite et al., 2009b) and negative ions (Coates et al., 2007) detected within Titan's upper atmosphere. These may allow, if oxygen is present in some free form, organic acid synthesis, potentially followed by formation of amino acids. Space environment radiation, including UV photons from the Sun, and energetic charged particles from the Saturn magnetosphere and interplanetary space, and GCRs contribute both to the production of the oxygen-rich magnetospheric plasma and to chemical evolution within Titan's upper atmosphere.

Well before the Cassini/Huygens mission arrival at Saturn, Raulin and Owen (2002) realized the seemingly unlikely prospect for free oxygen within Titan's dense N_2-CH_4 atmosphere and corresponding aerosols. As summarized in their Fig. 2, the O in amino acids is replaced with the "ammono" analog NH. If oxygen were to enter Titan's reducing atmosphere one would normally expect that it would rapidly react with methane to make CO and CO_2 gas (see Hörst et al., 2008). For the large ions observed by Waite Jr. et al. (2007) and Coates et al. (2007) these authors suggested that the dominant chemical pathway for making these heavy ions was formation of polycyclic aromatic hydrocarbons (PAHs), becoming PAHNs in the presence of nitrogen. Ali et al. (2015) have been studying the chemistry of cyclopropenyl cations where both cyclic and linear isomers can form in Titan's ionosphere. Coates et al. (2007) also showed evidence of mass 16 negative ions and suggested these could be thermalized O^- ions. Vuitton et al. (2009) reported on negative ion chemistry at Titan and suggested negative ions such as CN^-, C_3N^- and C_5N^-. Sittler Jr. et al. (2009a) noted that many of the reaction rates used by Vuitton et al. (2009) were only estimates and not measured. Vuitton et al. (2009) did use influx rates of keV O^+ lower than that reported by Hartle et al. (2006a, 2006b). Krasnopolsky (2012) found their model results compared better with observations when incoming O^+ ions from the magnetosphere were included.

Yelle et al. (2010) reported on Ion Neutral Mass Spectrometer (INMS) observations and theoretical calculations that supported presence of ammonia NH_3 in Titan's atmosphere with INMS-detected mass-18 ions identified to be $NH_4{}^+$ ions. But the Krasnopolsky (2012) model does not predict any $NH_4{}^+$ within Titan's ionosphere, so mass 18 might alternatively be H_2O^+? The recent analysis of the CAPS/ELS anion measurements clearly showed the presence of anion carbon chains composed of CN^- or C_2H^-, C_3N^- or C_4H^-, C_5N^- or C_6H^-, etc. Such molecular anions could develop into long carbon chains with N^- or H^- appendages, respectively. In addition, Desai et al. (2017) also noted that multi-charged negative states for fullerenes $C_{60,70}{}^{2-}$ would be stable (Wang and Wang, 2009). If so, $C_{60,70}{}^{-2}$ could produce the m/q peaks ~ 360–420 amu/q in the CAPS/ELS mass spectra shown in Fig. 2 of Desai et al. (2017) for altitudes between 950 and 1000 km.

There are further analogs to previous work on carbon chain formation in molecular clouds (MC) and planetary nebula (PN) (Herbst, 1981; McCarthy et al., 2006; Brünken et al., 2007; Remijan et al., 2007; Sakai et al., 2007, 2008; Thaddeus et al., 2008; Herbst and Osamura, 2008). These can then lead to formation of fullerenes (Thaddeus, 1994, 1995), and positive ion fullerenes possibly from MC or PN illuminated by strong UV starlight (Galazutdinov et al., 2000; Foing and Ehrenfreund, 1994, 1997; Campbell et al., 2015; Ehrenfreund and Foing, 2015). It is known from some astrophysical observations (Sellgren et al., 2010) that up to ~ 1% of interstellar carbon can be in the form of fullerenes.

Fullerenes at Titan's cold atmospheric temperatures T ~ 140 °K can condense into large clusters. Martin et al. (1996) produced fullerene clusters in an oven at T ~ 500 °C. In a cold helium gas surrounding the oven at T ~ 100 K the fullerenes come into contact with this helium gas and rapidly condense into aerosols with some over 100 C_{60} molecules or mass > 80,000 amu. The fullerenes in these experiments could be coated with alkaline metal atoms denoted as M = Ba, Li, Ca, K, and Na. They observed a spectrum of masses with localized peaks at 720 + 32 M (32 M-type atoms), 720 + 104 M, 720 + 236 M, and 720 + 448 M. These totaled in mass ~ 2000 amu, 4984 amu, 10,396 amu and 19,088 amu, respectively, in the case of Ca so the metal coated C_{60} became very large molecules. The experimenters were also able to dope the fullerenes with metal halides which become trapped inside the fullerenes. This raises the question of whether fullerenes could be doped with CO or H_2O within Titan's upper atmosphere as they are forming into fullerenes? In their laboratory Zhang et al. (1986) were able to show the C_{60} fullerenes, which are nearly perfectly closed, were inert to the reacting molecules NO, H_2, CO, SO_2, O_2 and NH_3.

Zhang et al. (1986) and Kroto and McKay (1988) provided evidence for very large onion fullerenes or what some call carbon nano-onion (CNO) molecules. These onion fullerenes can be found in carbonaceous chondritic meteorites (Becker et al., 2006). Kroto and Mckay (1988) argue that the fullerenes can grow into larger quasi-single crystal particles which have a concentric spiral-shell internal structure like onion fullerenes. The sub-structure of fullerenes is planar carbon pentagons which provide the necessary curvature for fullerene formation. The primary CNO-formation mechanism occurs when closure to form C_{60} is supposed to occur, but does not, so unclosed shells instead form and allow for larger particle growth with multiple shells (i.e., onion fullerenes or CNOs). They further argue that the growth rate from accreting carbon molecules is proportional to the CNO area so as the particle grows in size the accretion process will accelerate until some rate-limiting process occurs. Molecule sizes up to C_{240} and C_{540} were reported by Kroto and McKay (1988) with cross-sectional area ~ 10 times larger than C_{60} or outer diameters ~ 140 Å or 14 nm.

In the papers by Thaddeus (1994, 1995) about molecular clouds, they note observational evidence for long carbon chains that tend to maximize in size at ~ 40 carbon atoms. Longer carbon chains > 40 carbon atoms will then fold into fullerenes which are more stable against breakup by various processes (i.e. photocleavage, photodissociation, etc.). The proposed dominant process for growth from accreting molecules is C^+ insertion followed by non-dissociative electronic recombination. Then once the fullerenes have formed they will continue to accrete carbon indefinitely until they become very large amorphous carbon grains. In addition Garcia-Hernández and Diaz-Luis (2013) observed the Diffuse Interstellar Band (DIB) at 4428 Å which could be produced by the CNOs, C_{240} and C_{540} or the larger fullerenes C_{80} and C_{320}.

In the case of Titan's ionosphere and thermosphere, methane is in abundance and one might expect them to interact with the newly formed fullerenes. In this case methane molecules become the accreting particles and since the atmosphere is very cold with T ~ 140 K the methane will have low energy collisions with the fullerenes which should increase likelihood of sticking. Considering how fullerenes can stick together and form larger aerosols and grow into larger molecules, although speculative, one might expect them to also interact and combine with PAHs and PAHNs, and then form into even larger aerosols that are composed of HCNO.

Further justification for the growth of fullerenes within Titan's atmosphere, and subsequent trapping of oxygen ions, can be found in the laboratory analysis of carbonaceous chondritic meteorites wherein noble gases are found trapped in meteorites containing carbon rich, acid resistant residues (Lewis et al., 1975; Heyman, 1986; Becker et al., 2006).

Here we note, there is both experimental and theoretical evidence by Kaiser et al. (2013) that methane molecules will stick to fullerenes as the accreting gas for multilayer fullerene formation. They studied the adsorption of methane molecules upon aggregates of fullerenes $(C_{60})_m$ (i.e., monomers m = 1, dimers m = 2, etc. to m = 5) with closed shells and no defects. Using liquid helium nano-droplets that passed through vacuum ~ $1-4 \times 10^{-3}$ Pa pickup region of methane gas with either C_{60} or C_{70} vapor followed by electron impact ionization and time-of-flight mass spectrometer measured the mass spectrum of the fullerene-methane molecules $(C_{60})_m(CH_4)_n$. The mass spectrum was composed of peaks at $n = 1,2,3$, etc. with a power law decrease with particle mass. In the case of the fullerene monomer an anomalous peak occurred at $n = 32$ while for the dimer at $n = 56$. Based on theoretical calculations at assumed T ~ 4 K for the C_{60} monomer an inner layer with ~ 32 CH_4 molecules would form at radial distance r ~ 7 Å with binding energy ~ 0.2 eV and second layer would form with ~ 80 CH_4 molecules, radial distance r ~ 9 Å and binding energies < 0.1 eV. For dimers, trimers etc. at the fullerene interfaces the methane binding energies were greater. Kaiser et al. (2013) also noted at sites where defects might occur such as for carbon nanotubes the molecular adsorptions would be greater, so one might expect this to occur at unclosed fullerene shells so onion fullerene formation could occur at Titan. They studied the structure of the methane molecules around a fullerene dimer with temperature which was highly structured at T ~ 10 K, while less structured at T ~ 40 K. Although Titan's ionosphere-thermosphere is ~ 140 K, as the fullerenes are forming the shells will not be complete so onion fullerenes might still form. But we are not aware that the experimental formation of onion like fullerenes within a cold methane gas at T ~ 140 K has been done.

2. Revised estimates of atomic oxygen concentrations trapped within Titan aerosols

In this section we consider the charge states of fullerenes and what one might expect these to be at Titan. Titan is relatively far from our Sun with relatively cold atmospheric temperatures $T < 180$ K and ionospheric electron temperatures ~ 1000 K, so ion/neutral ratios are quite small. The model calculations by Vuitton et al. (2009) for Titan's ionosphere give anion/neutral ratios 10^{-2} to 10^{-5}. Sittler Jr. et al. (2009a) predicted O abundance within aerosols ~ 7.0×10^{-6} by using the negative ion abundances from observations of Coates et al. (2007). Liang et al. (2007) reported aerosol densities ~ 10^4 particles/cm^3, while Coates et al. (2007) reported lower densities ~ 200 anions/cm^3. The anion/neutral ratio is then 2%, consistent with the majority of fullerenes being neutral as found (Garcia-Hernández and Diaz-Luis, 2013) in planetary nebulae and in related model calculations. We note, that Lavvas et al. (2013) came to a different conclusion with neutral aerosol densities ~ anion densities between 900 km and 1000 km and found total aerosol densities ~ 4000 particles/cm^3 < 10^4 particles/cm^3 at 1000 km. Their model only considered PAHs and not fullerenes.

Sittler Jr. et al. (2009a) estimated an aerosol mass flux $\Phi \sim 2.7 \times 10^{-14}$ kg/m^2/s for which we now prefer $\Phi \sim 1.3 \times 10^{-14}$ kg/m^2/s. Our revised estimate will increase to $\Phi \sim 6.7 \times 10^{-13}$ kg/m^2/s (near the upper limit by Borucki et al. (2006)) if one multiplies it by 50, our estimated neutral/anion fullerene abundance ratio. If one divides this new mass flux by the intermediate mass flux of Borucki et al. (2006) which is $\Phi \sim 4 \times 10^{-13}$ kg/m^2/s, then the fullerenes can be > 100% of the aerosol mass with the atomic oxygen molar fraction ~ 10^{-5} within each aerosol. We estimate the O molar fraction within each aerosol by first estimating the "effective" optical depth τ of the fullerenes to the incoming keV O^+ ions. The seed particle cross-section is $\sigma_{seed} = \pi r_{seed}^2 = 2.54 \times 10^{-14}$ cm^2. It is estimated by first assuming the seed particle mass M_{seed} ~ 4000 amu and dividing it by the C_{60} mass which is $M_{C60} = 720$ amu to give us ~ 6 fullerenes per seed particle. We further assume the seed particles are spherical with radius $r_{seed} \sim 5\text{Å}*(6)^{1/3} \sim 9$ Å, given the fullerene radius ~ 5 Å. Then the optical depth $\tau = \sigma_{seed}*N_{seed}*H = 0.15\%$, where the seed particle number density $N_{seed} = 10^4$ #/cm^3 and the atmospheric scale height H = 60 km. This means ~ 0.15% of incoming O^+ ions could be trapped within a seed or embryo particle (note, even though the seed particles get bigger below 950 km, the penetration of the keV O^+ to lower altitudes decreases). Therefore, > 99% of the O still goes into making CO as modeled by Hörst et al. (2008) and thus not violating their CO calculations. Then as the seed or embryo aerosols drop to lower altitudes they will condense together while preserving the fraction of seed particles with oxygen ~ 0.15%. When comparing the number of O atoms relative to the "effective" number of acetonitrile CH_3CN with mass ~ 41 amu as used by Hudson et al. (2008), there will be ~ 4000 amu/41 amu ~ 100 of the acetonitrile per seed particle, so then the fraction of atomic oxygen ~ 0.0015% by number or mole fraction. This is close to the estimated upper limit of water contamination in the irradiated methyl ices used in the Hudson et al. (2008).

3. Growth of Fullerenes into aerosols for heights > 950 km: Is it fast enough?

Sittler Jr. et al. (2009a) estimated for altitudes ~ 1000 km that the fullerenes should fall with velocity v ~ 10 m/s with precision no better than a factor of 2. At these relatively high fall velocities one might initially think that fullerenes cannot condense into embryo sized aerosols within one scale height H ~ 60 km or H/v ~ 6000 s. If one just considers the collisions between fullerenes to be the dominant process, the ratio $\lambda_{mfp}/H \ll 1$ must be true for aerosol formation. Since, the mean free path $\lambda_{mfp} \sim 1/(n\sigma)$ with $n \sim 10^4$ C_{60}/cm^3 and $\sigma \sim \pi(2r_F \sim 10\,Å)^2 \sim 3 \times 10^{-14}\,cm^2$ and with H ~ 60 km the ratio becomes $\lambda_{mfp}/H \sim 555 \gg 1$ (i.e., fullerenes fall like rocks). But, if fullerene growth into onion fullerenes or CNOs from methane impact is important along with increase in particle size, then aerosol growth becomes more probable. As noted previously, based on the work by Kaiser et al. (2013) there is experimental and theoretical evidence that this would occur. In the case of fullerene growth, $n \sim 2 \times 10^8$ CH_4/cm^3 and $\sigma \sim 4\pi r_F^2 \sim 6 \times 10^{-14}\,cm^2$ (i.e., assume fullerene has on average grown an addition shell for C_{240}) and the thermal speed of methane molecules is $w_{CH4} \sim 3.8 \times 10^4$ cm/s which gives collision frequency $\nu \sim n\sigma_F w_{CH4} \sim 1$ cps. If it takes ~ 6000 s to fall one scale height then there will be $\sim 6 \times 10^3$ CH_4 collisions with the CNO, which is more than enough to produce C_{540}. Of course, this assumes no interaction with the larger area planar PAHs and PAHNs that are likely forming in the same region. Once these larger fullerenes or CNOs start sticking together they become even larger, so their cross-sectional areas increase > ×4 so the process becomes exponential as shown in Fig. 2 from Coates et al. (2009) and gives further support to the original paper by Sittler Jr. et al. (2009a).

Within these aerosols amino acids could be produced from exogenic sources of energetic radiation in the atmosphere including solar UV photons, magnetospheric MeV electrons, and the more-penetrating galactic cosmic rays. One can show that GCRs provide the greatest potential for the conversion of the accumulated aerosols onto Titan's surface into tholins and/or prebiotic molecules such as amino acids. Laboratory experiments do show amino acids forming in materials composed of methyl ice with traces of water (i.e., $H_2O \sim 10^{-5}$ estimated abundance) when irradiated by MeV protons for accumulated dose ~ 60 Grads (Hudson et al., 2008) which is then followed by hydrolysis of the irradiated samples. At this dose essentially, all molecular bonds are broken and then reform into modified species.

4. Galactic cosmic ray model of Titan and exobiological molecule production at Titan

If the aerosols accumulated onto Titan's surface are enriched with atomic oxygen as discussed in the previous sections, one must also identify an energy source of sufficient intensity that can convert the surface coated veneer of HCNO composed aerosols into tholins and organic molecules such as glycine and other amino acids. We have identified galactic cosmic rays and their secondary interaction products as the prime energy source since the GCR can penetrate down through Titan's dense atmosphere and produce highly penetrating secondaries such as muons that reach the surface and sub-surface at ~ 100 m depths. In our model the atmosphere is composed of N_2 with mole fraction ~ 98.5%, CH_4 with mole fraction ~ 1.48% except near surface where it rises to ~ 5.65% with N_2 ~ 94.35% and no argon since the mole fractions of ^{36}Ar and radiogenic ^{40}Ar are $(2.1 \pm 0.8) \times 10^{-7}$ and $(3.39 \pm 0.12) \times 10^{-5}$, respectively. The mole fractions are based on the experimental results by Niemann et al. (2010) below 400 km altitude. The model atmosphere is split vertically into 21 horizontal layers by the approach of the atmospheric model of Borucki et al. (2006) and using densities from Yelle et al. (1997). With regard to Titan's surface and sub-surface it is assumed to be primarily water ice with mass density ~ 1 g/cm^3.

Fig. 1 shows the GCR spectrum from 1 MeV to 1 TeV. They come from both interplanetary space and galactic space and is compared to long term averages of proton fluxes from the Pioneer 10 and 11 Cosmic Ray Telescopes (CRT), the Voyager 1 and 2 Cosmic Ray Sensors (CRS), and from the Advanced Magnetic Spectrometer 2 (AMS-2) on the International Space Station (ISS). The Pioneer and Voyager fluxes are averaged over years when the spacecraft were at 5–20 AU in the middle heliosphere, Saturn being at 10 AU, while the ISS is in low Earth orbit. Also shown are the model spectra as a function of solar activity from fits to high-energy cosmic ray data by Potgieter et al. (2015). The Pioneer 10, AMS-2, and Potgieter-Voss solar minimum data are in closest agreement to our flux model, while the Voyager data show stronger response to solar modulation below 200 MeV. As we will show, the secondary energy fluxes at Titan's surface are dominated by primary protons well above a GeV, thus we take the model flux spectrum for energies between 10 GeV and 1 TeV as a reasonable approximation for our GCR interaction simulation. Lower energy, 10–10^4 MeV, protons incident onto Titan's atmosphere will be more relevant to Titan's upper atmosphere.

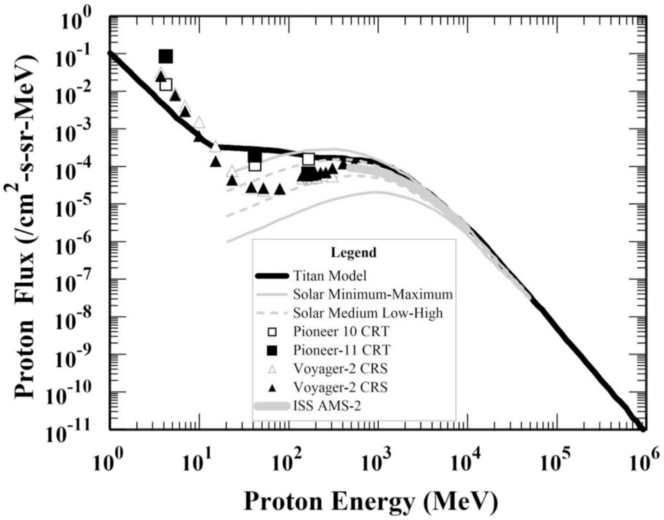

Fig. 1. Comparison of our proton flux model (black solid curve), used to generate the simulation results in Fig. 2, to the Advanced Magnetic Spectrometer 2 (AMS-2) spectrum (thick grey curve, averaged for May 20, 2011 to April 13, 2017) from the International Space Station, the solar modulated spectra (light solid and dashed curves) from Potgieter et al. (2015), for which higher flux arises from lower modulation related to lower solar activity, and Pioneer and Voyager fluxes averaged over 5–20 AU. The Pioneer 10&11 and Voyager 1&2 averaging dates are: P-10 Cosmic Ray Telescope (CRT, open box), Nov. 24, 1973 to Oct. 24, 1979; P-11 CRT (solid box), April 18, 1977 to Jan. 9, 1986; V-1 Cosmic Ray Subsystem (CRS, open triangle), Jan. 19, 1979 to June 19, 1984; V-2 CRS (solid triangle), April 23, 1979 to May 25, 1986.

As mentioned earlier, previous GCR models such as that by Molina-Cuberos et al. (1999) were more concerned with ionization of Titan's lower atmosphere. In order to extend our own results through the atmosphere to the sub-surface, we have utilized a GEANT (GEometry ANd Tracking) based model (Brun et al., 1994), as most recently described in Cooper and Sturner (2018), which here we refer to as MGEANT/GCALOR. MGEANT (Sturner et al., 2000) does the setup of beam and target geometries, tracks trajectories and energy losses for all shower generations and handles electromagnetic interactions, while GCALOR (earlier called CALOR) deals only with the hadronic interactions. Battistoni et al. (2003) tested the high-energy (GeV to TeV) FLUKA component of GCALOR for secondary production in atmospheric showers generated by GCR protons and found general uncertainties to be < 20%. Results of earlier tests for GEANT/CALOR application to hadronic production in calorimeter tests were discussed by Zeitnitz and Gabriel (1994) with similar uncertainties.

The MGEANT/GCALOR code was only setup to run for GCR protons, so we compute only a lower limit to dosage rates. With inclusion of dosages from all ions heavier than protons, e.g. from helium through iron, and accounting for higher biochemical efficiency of heavier ions, the total dosage rates could be several times higher. For comparison to measurements at the Mars surface below its thin atmosphere, Matthiä et al. (2017) computed quality factors of 1.54 to 3.14 from several different radiation-transport codes, while the Mars Science Lander Radiation Detector (RAD) directly used linear-energy-transfer (LET) data to find a value of 2.62. But Titan GCR shower fragmentation into lighter

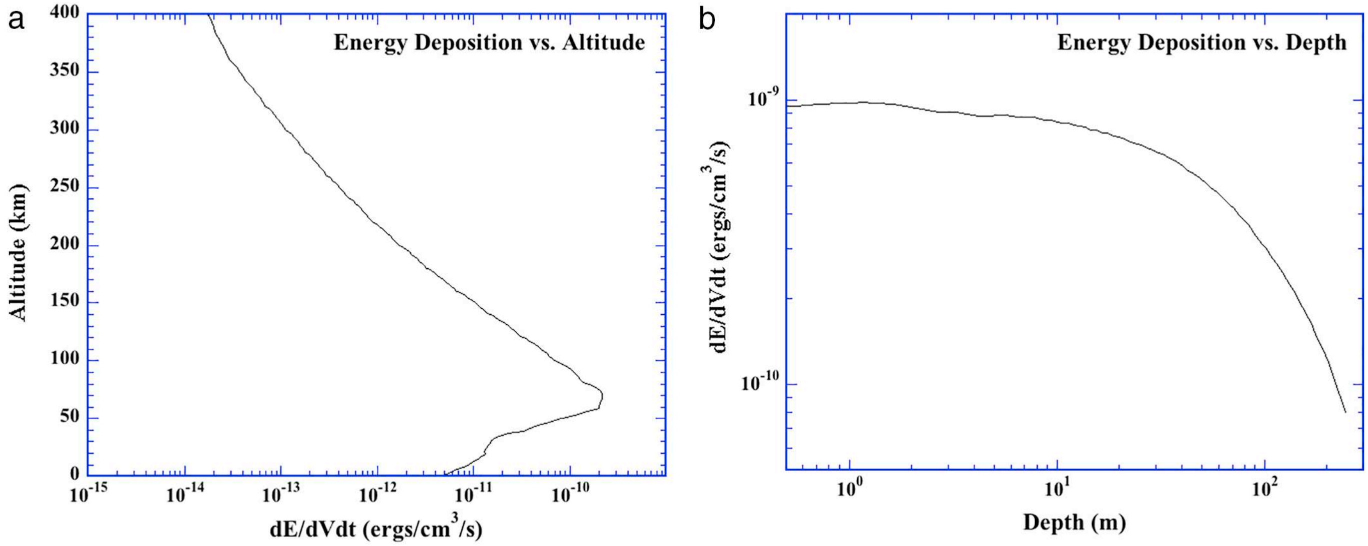

Fig. 2. a. GCR energy deposition rate in ergs/cm^3/s as a function of altitude in Titan's atmosphere, as computed from the incident proton model spectrum in Fig. 1 and the MGEANT/GCALOR radiation transport code.
b. GCR energy deposition rate as a function of depth below the water/ice surface, also computed from the model spectrum of Fig. 1 and the MGEANT/GCALOR code. The sudden jump in energy loss near the surface when compared to Fig. 2a is due to the sudden jump in mass density from 0.00544 g/cm^3 for the atmosphere to 1 g/cm^3 for the sub-surface.

particles at large depths would reduce the quality factor unity for electrons, muons, and gamma rays while secondary neutrons, pions and protons do not reach the surface. We assume that the total correction factor for heavier ions and quality factor could be a factor of two, so the upper limit on the actual dosages could be two times higher than our computed lower limit with MGEANT/GCALOR.

A dosage rate vs. depth profile of the GCR interaction with Titan's atmosphere is shown in Fig. 2a, the surface and sub-surface rates being shown in Fig. 2b. Some of the characteristic results of the model are summarized in Table 1. The atmospheric slices are planar with sufficient horizontal extent to contain trajectories of all primary and secondary particles from isotropic incidence onto a spot at the top of the atmosphere. The code includes interactions and energy deposits from protons, neutrons, electrons, positrons, pions, muons, gamma rays and more exotic but short-lived particles. Neutrinos are also produced from charged pion and muon decays but generally escape from the model target volume without interaction. The mean energy of primary cosmic ray protons at the top of the atmosphere that produce significant energy deposits below the ice surface through their secondary particles (i.e., primarily muons and their products) and photons is $\sim$ 334 GeV. Note, we did complimentary simulations that showed the main component of the shower at subsurface depths were muons and photons. At $\sim$ 100-m depth in the surface ice or at the bottom of surface lakes the energy deposition is dominated by ionization energy losses of secondary particles originating from cosmic ray proton interactions at even higher energies. The incident cosmic ray fluxes at energies $> >$ 10 GeV are relatively constant with no significant variation from cosmic ray modulation by the solar wind magnetic field that varies on decadal time scales.

Table 1
Results of the GSFC GCR model of Titan: 800,000 primary protons (GEANT3 code used).

Item	Water
Total input energy in keV (%) from 800,000 primary GCR protons	1.99×10^{13} (100%)
Total shower energy in keV (%) deposited in the atmosphere	1.17×10^{13} (59%)
Total shower energy in keV (%) deposited in the surface	8.24×10^{10} (0.4%)
Total shower energy in keV (%) lost to neutrinos	7.16×10^{12} (36%)
Total shower surface energy flux (erg/cm^{2}s) deposited into the surface volume.	8.01×10^{-6}

Notes
1. The integral GCR proton flux in the first row is $J_0 = 1.15 \times 10^{-2}$ p/cm^2-s-sr from 10 GeV to 1 TeV. The number of incident GCR protons is $N_0 = 800{,}000$.
2. The top of the atmosphere is assumed to be planar, so the surface flux there is $\pi J_{CR} = 3.61 \times 10^{-2}$ p/cm^2-s in the downward direction onto a circular spot of radius 100 cm and area A.
3. For flux normalization the time duration of the irradiation by all primaries is $\tau = 705.4$ s as computed from $\tau = N_0/(J_0 \pi A)$. The total shower surface energy flux was calculated by dividing the total shower energy deposited in the surface by 705.4 s, and the illuminated spot area = $\pi \times 10^4$ cm, and then multiplying by the ratio of the surface area of the top of the atmosphere and the area of Titan's surface.
4. The average energy of a primary proton ultimately producing non-zero energy flux at the surface is 334 GeV.

Dose time scales are 100 Myrs to 4.5 Gyrs for accumulation of 29.99 krad – 1350 krad at the surface. Referring to Table 16.2 in Sittler Jr. et al. (2009b), the energy inputs from solar UV and GCR are similar (see also Robertson et al., 2009 for solar UV fluxes). The solar UV deposits mostly at heights > 400 km while the GCR energy deposition peaks deeper into the atmosphere at altitudes $\sim$ 100 km. Since it takes only $\sim$ 1000 years for the aerosols to settle down to Titan's surface the chemical processing of the aerosols within the atmosphere is not significant. In the case of magnetospheric particles, which can penetrate down to only 800 km altitudes, the ionospheric residence time scale of the observed aerosol embryos by Coates et al. (2007) are only 12 h (Sittler Jr. et al., 2009a), The total accumulated dose due to solar UV and magnetospheric particles is therefore negligible at $\ll$ 1 rad.

The radiation model predicts total dose rates $\sim 10^{-11}$ rads/s at the surface for atmospheric tholins with mass density $\rho \sim 1.0$ g/cm^3 (Hörst and Tolbert, 2013) while others such as Khare et al. (1994) used 1.5 g/cm^3. Using $\rho \sim 1$ g/cm^3 the accumulated depth of tholins at the surface is $\sim$ 15 m. The surface tholin accumulation comes from the maximum aerosol mass flux $\Phi \sim 10^{-12}$ kg/m^2/s over a surface age of 450 Myrs. The average surface radiation dose to fifteen meters depth over this time period is $\sim$ 135 krad.

The GCR interaction products produce significant energy deposition down to $\sim$ 100 m below the icy surface. In the methane-ethane lakes at fluid density $\sim$ 0.45 g/cm^3 (Lorenz et al., 2003) this corresponds to penetration down to ~ 200 m depths. Recently, Cassini radar altimetry data was used to estimate the depth of Titan's large sea Ligeia Mare which was found to be ~ 150 m (Mastrogiuseppe et al., 2014). Therefore, the GCR-produced radiation should be able to penetrate down to the lake bottoms where sediments can accumulate. Here we note, that the radar altimetry results also required the lake to be very clear with little sediments and nearly pure methane, which means the aerosols or sediment specific gravity must be $> 0.45\,g/cm^3$ in order to sink to the bottom. Note, Lorenz (2014), who studied Titan's dunes, used mass density $\sim 1\,g/cm^3$ for the dust particles while $\rho \sim 1.65\,g/cm^3$ applies for fullerenes.

Cosmic ray interactions with Titan's lakes are very intriguing since they should penetrate to the bottom of these lakes and process any of the sediments accumulating over the bottom of such lakes. The lakes can be reservoirs for transient river runoff whenever methane clouds and storms form (i.e., flash flood scenarios) and as estimated by Hayes et al. (2008) the timescales of lake drainage are ~ 10 years when considering evaporation and seasonal changes (i.e., Titan year ~ 29 Earth years). Subsurface and surface drainages can fill lakes (Stofan et al., 2007) and longer timescales may then be expected.

The original lake model with karstic processes is the more likely explanation, where depressions are formed by surface material dissolution by methane/ethane liquids (see Jaumann et al., 2009a and Cornet et al., 2015). At present, it's not clear if the aerosols/tholin materials will be immiscible with methane/ethane liquid lakes but if so then sediments can accumulate on the bottom of Titan's lakes. The composition of the organic materials may be more diverse than the sediments for an isolated lake. If one uses the max mass flux of aerosols estimated by Borucki et al. (2006) which is close to our revised estimate here $\sim 10^{-12}\,kg/m^2/s$, and uses tholin mass density $\rho \sim 1000\,kg/m^3$ and time scale $\tau \sim 4.5 \times 10^8$ years, we compute the resulting mean depth of tholins to be ~ 15 m. Assuming the surrounding areas drain into the lake is considered then sediment thicknesses can be > 15 m. The lifetime of lakes compared to the ~ 450 Myr timescales is unknown but estimates as short as 10 years have been made (Hayes et al., 2008), so one would expect lakes or seas would come and go over 450 Myr timescales, so the accumulated sediments at the bottom of lakes could contribute to enriched layers of tholin materials within the near surface sub-layers of Titan.

Hudson et al. (2008) showed that G-factor ~ 0.001 applies for Glycine production by irradiation of methyl ice samples, which means that one Glycine molecule is produced for every 10^5 eV of deposited energy. They used pure Acetonitrile CH_3CN ices with very small water levels ~ 0.001% for O. For G ~ 0.001 and GCR surface energy flux noted above at Titan's surface down to ten meters depth of tholin accumulation we estimate as a lower limit the abundance levels ~ 2.5 ppb of amino acids such as Glycine over 450 Myr period, the upper limit with addition of heavy GCR ions and biochemical quality factors then being ~ 5 ppb. Therefore, we conclude that this synergy of Saturn system, exogenic irradiation, and molecular processes provide a potential pathway for accumulation of prebiotic chemicals onto the surface of Titan. Since fullerenes are also thought to exist in interstellar space, similar processes may also occur there to seed molecular clouds with prebiotic chemical species yet to be determined.

5. Two-step process for making amino acids: GCR irradiation and large meteor impacts

Hudson et al. (2008) irradiated CH_3CN with estimated trace levels of water ice ~ 0.001% which is similar to the oxygenation levels we're proposing here. So, it had all the ingredients, methyl CH_3 and the nitrile CN, for making amino acids. Elsila et al. (2009) investigated the chemical pathways of similar ices to amino acids using UV photolysis but also had to use hydrolysis to convert precursors to amino acids. The Huygens probe Gas Chromatograph Mass Spectrometer, GCMS, near and on the surface of Titan (Niemann et al., 2010) detected CH_4 at enhanced levels along with evidence the surface may have been wet with liquid methane (see Niemann et al., 2005, 2010; Zarnecki et al., 2005). H_2 gas was surmised to be coming out of the surface at the 0.001 mol fraction level, indicative of H_2 as a considerable component, and trace levels of acetylene C_2H_2, cyanogen C_2N_2, benzene and CO_2 were also observed at and near the surface. This indicates, that the surface is likely composed of GCR irradiated aerosols, converted into tholins, amino acids and their precursor molecules, with all the required ingredients theorized above. In addition, if one has a subsurface water ammonia ocean, then within the localized regions where cryovolcanism is occurring (Jaumann et al., 2009a; Lopes et al., 2013), liquid mixtures of water and ammonia would come into contact with the precursor molecules produced by GCR irradiation one would expect them to be converted into amino acids. In the lab environment acids such as HCl are used during the hydrolysis process as a catalyst to speed up the reaction rates while at Titan with longer time scales such catalysts are not required. Impact sites (Lorenz et al., 2007; Wood et al., 2010; Neish and Lorenz, 2012; Neish et al., 2016) may also be regions where amino acids are forming from hydrolysis where the ice crust is temporarily converted to liquid water. Using cratering rates based on crater counts for Rhea and Iapetus (Fig. 4 from Lorenz et al., 2007) and images of craters on these bodies (Jaumann et al., 2009b) we estimate ~ 100% of Titan's spherical surface would have received impacts with craters > 10 km diameters. As discussed in Jaumann et al. (2009b) Titan's surface is completely modified over a period ~ 1 Gyrs with crater remnants of past bombardments totally erased from the surface, by the accumulative effects of aerosols and by cryovolcanic, Aeolian, fluvial, tectonic and karstic processes which are expected to be constantly at work (see discussions below). This means that a large portion of Titan's leading and trailing hemispheric surfaces could be composed of amino acids as proposed here.

We have computed that energetic cosmic rays > ~ 350 GeV incident at the top of the atmosphere are required to produce significant energy deposition at the surface below Titan's dense atmosphere with $\sim 10^4\,g/cm^2$ column mass density, the secondary flux at the surface coming mostly from energetic secondaries that can penetrate even further to 10^2-m depths. The importance of GCR radiation on the surface relative to the atmosphere can be traced to the very long time scales for exposure on the surface and sub-surface. Only ~ 1000 years is required for the aerosols to fall through the atmosphere and reach the surface, while ~ 450 Myrs is needed to process the aerosols on the surface to convert them to tholins and exobiological molecules. We estimate that the aerosols receive ≪ 1 rad dose within the atmosphere, while ~ 142 krad dose (i.e., heavy ions excluded) is accumulated on the surface after ~ 450 Myrs. Over the 450 Myrs surface age, geological processes will have buried the surface veneer of tholins over shorter times. Due to Titan's thick atmosphere the surface is likely not gardened by meteoritic impacts down to ~ 10 m depths except by larger impacts with diameters > 10 km (see Neish and Lorenz, 2012). The actual number of observed large and small craters from meteor impacts are smaller than expected since they are covered by the falling aerosols from Titan's atmosphere discussed here, and otherwise modified by Aeolian, fluvial, tectonic and volcanic processes. Therefore, the geological time scales for Titan are estimated to be short at ~ 1 Gyr (Jaumann et al., 2009a; Wood et al., 2010; Porco et al., 2005; Lorenz et al., 2007; Lunine, 1990; Neish et al., 2016) but specific areas could have lifetimes shorter/longer than this estimate with lakes likely to be the shortest-lived regions. Since the energy deposition from cosmic ray interactions can penetrate down to depths $\sim 10^2$ m in surface ice and the lakes, tholin processing could continue over periods > 450 Myrs so amino acids like glycine and its precursor molecules could accumulate.

6. Comparison of Titan glycine abundances relative meteorites, comets and molecular clouds

Here we compare our Titan glycine abundance levels relative to that observed in carbonaceous chondritic meteorites (Kvenvolden et al., 1970; Engel and Nagy, 1982), cometary dust particles estimated from the Stardust mission and upper limits of glycine measured within our galaxy's molecular clouds. Ehrenfreund et al. (2001) found from carbonaceous chondritic meteorites glycine at 600 to 2900 ppb levels, while Oro et al. (1971) detected glycine abundance ~ 5.3 μg/g by weight. If H is the dominant component of meteorites (Anders and Ebihara, 1982), then we estimate that the molar fraction for glycine is ~ 70 ppb; the different values could be traced to the different methods and definitions used. In the case of comets, the Stardust mission results by Elsila et al. (2009) give abundance ~ 2–34 pmol/cm^2 but the molar fraction of the cometary dust was not given. In the case of molecular clouds Kuan et al. (2003) reported column density abundances of glycine relative to H_2 to be ~ 0.2 to 1.5 ppb, but Snyder et al. (2005) said not all lines were observed. So, assuming a possible detection the abundance levels are likely < 0.2–1.5 ppb. So, this gives us a broad range of abundance levels for which our estimate for Titan is at intermediate levels.

7. Conclusions

The reducing hydrocarbon-rich nitrogen atmosphere of Titan with some contributing external energy inputs from solar UV, upstream plasma ions and electrons, energetic particles and GCRs, along with the entrapment of magnetospheric oxygen ions in fullerenes could allow exobiological reactions and their products such as amino acids to accumulate on Titan's surface and within its sub-surface. As noted above, several key discoveries by Cassini had to be made before such a synergistic picture could be constructed. These are: 1) discovery of water group ions throughout Saturn's magnetosphere from inside Enceladus' orbit to outside Titan's orbit: 2) discovery that the magnetospheric oxygen ions at Titan had energies > 1 keV: and 3) the discovery of large positive and negative ions within Titan's upper atmosphere for heights > 950 km. In addition, several key conceptual models and data analysis results have also contributed such as: 1) transport of fast neutrals to Saturn's outer magnetosphere as developed by Johnson et al. (2005, 2006a, 2006b): 2) the analysis of the CAPS/ELS observations of anions in Titan's thermosphere-ionosphere first done by Vuitton et al. (2009) and later more precisely the analysis by Desai et al. (2017) have shown evidence of negatively charged long carbon chains that could eventually grow into fullerenes: 3) the realization by Sittler Jr. et al. (2009a) that the heavy negative ions could be fullerenes capable of trapping keV oxygen ions from the magnetosphere: and (4) that the fullerenes can condense into larger molecules and clusters of fullerenes and combine with PAHs and PAHNs to make the aerosols with free oxygen inside. These aerosols could then be irradiated by GCRs to make amino acids within the aerosols residing in the atmosphere, on the surface and sub-surface, including within Titan's lakes and lakebeds. There is a lack of complex molecules with oxygen within Titan's atmosphere except for the simple molecules CO and CO_2. So, if oxygen is present, we suggest that it could be trapped within the aerosols.

The addition of our GCR model to Titan's atmosphere, surface and sub-surface has allowed us to quantitatively close the loop on this discussion with the formation of exobiological molecules on the surface such as the amino acid glycine with abundances ~ 2.5–5 ppb over a 450 Myr time scale, but as previously noted it is a two-step process to make amino acids, radiation plus hydrolysis. The GCR irradiation makes the precursor exobiological molecules while the hydrolysis process is provided by large meteor impacts upon Titan's surface over ~ Gyr time periods to convert the precursors to amino acids.

We also revised upward the contribution of fullerenes within the aerosols from ~ 6.8% to nearly 100% for fullerenes, with trapped atomic oxygen abundance levels of ~ 10 ppm by number and downward mass flux levels near the maximum level of $\Phi \sim 10^{-12}$ kg/m^2/s. Using the observed number of 12.5 nm size aerosols ~ 10^4 /cm^3 from Liang et al. (2007), who used UVS data and the maximum anion density ~ 200 anions/cm^3 estimated by Coates et al. (2007), the ratio 200/10^4–2% for anion/neutral ratio. This is consistent with theoretical estimates of molecule sized anion abundances by Vuitton et al. (2009) with anion/neutral ratios < 10^{-2} and recent observations of planetary nebula, PN, where both neutral fullerenes and PAHs are observed (Otsuka et al., 2013). This is important since now oxygen abundances within the aerosols could be close to those used by Hudson et al. (2008) irradiation studies.

The Vuitton et al. work focused on the formation of negative ions and growth of large molecules such as PAHs. Desai et al. (2017) showed evidence for anion carbon chains. Sittler Jr. et al. (2009a) made the case for long carbon chains (unsaturated) and fullerenes, while in this paper we have shown that fullerenes can rapidly grow into large multi-shelled onion fullerenes or ofton called CNOs. The growth of these large molecules with methane as the assumed dominating accreting gas, has quantitatively shown such large molecules, C_{240} and C_{540}, can rapidly form in Titan's thermosphere-ionosphere, resolving the production rate issue only alluded to by Sittler Jr. et al. (2009a). In order to make further progress and quantify the different chemical pathways, e.g. for formation of PAHs vs fullerenes, one needs to measure the reaction rates for the polymer precursors such as the ethyl radicals C_2H and cyanogens CN as prime examples. We propose the CRESU facility in Rennes France (Morales et al., 2010; Ali et al., 2013) for measuring such reactions rates at the cold temperatures characteristic of Titan T ~ 100–200 K and even colder for dense molecular clouds T ~ 10–30 K (see Kaiser et al., 2013). In addition, we propose a measurement concept using the Goddard facility to measure the capture of oxygen ions ~ 400 eV within fullerenes (Sittler, 2010; Ali et al., 2010). Like that done by Weidinger et al. (1998) for nitrogen capture in fullerenes, electron paramagnetic resonance (EPR) technique would eventually be needed to study the stability of oxygen within a fullerene. We would like to have experiments performed where fullerenes with defects are injected into a cold methane gas with T ~ 140 K to check for large molecular growth. To the best of our knowledge this has not been done. Finally, with regard to future missions to Titan's surface, the best place to look for glycine and other amino acids is in the vicinity of relatively young craters before these acids can be buried by younger aerosol/tholin materials. If the mass density is ~ 1 g/cm^3 for tholin material, then we estimate ~ 15 m / 450 Myrs ~ 3.3 cm/Myrs of tholin material. For crater age ~ 1 Myrs one might see the amino acids at a depth > 3.3 cm, while the precursor molecules might be seen at shallower depths. Other possibilities are river channels where erosion has exposed the older layers or regions where cryovolcanism is thought to be occurring now or in the recent past.

Acknowledgements

This work was supported at NASA Goddard Space Flight center in part by the Cassini Plasma Spectrometer (CAPS) Project through NASA Jet Propulsion Laboratory contract 1243218 with the Southwest Research Institute in San Antonio, Texas. The remainder was provided by the Solar System Exploration Division, GSFC 690 Exosphere-Ionosphere-Magnetosphere Modeling (EIMM) program. The Pioneer 10 &11 CRT, Voyager 1&2 CRS, and ISS AMS-2 proton flux data in Fig. 1 are from NASA's Virtual Energetic Particle Observatory (VEPO) at http://vepo.gsfc.nasa.gov/, as earlier submitted to the NASA Space Physics Data Facility by the corresponding instrument teams. The responsible principal investigators of those teams are as follows: CRT, the late Dr. Frank McDonald of the University of Maryland at College Park; CRS, Dr. Edward C. Stone of the California Institute of Technology; AMS-2, Dr. Samuel C. Ting of the Massachusetts Institute of Technology.

References

Ali, A., Chornay, D., Sittler Jr., E.C., Canosa, A., 2010. Gas-phase prebiotic chemistry on

Titan:specific laboratory kinetic measurements on the formation rates and mechanisms for molecular anions observed by the Cassini mission. In: Proceedings of the Titan Through Time: a Workshop on Titan's Formation, Evolution and Fate. NASA,Goddard Space Flight Center, pp. 79.

Ali, A., Sittler Jr., E.C., Chornay, D., Rowe, B.R., Puzzarini, C., 2013. Cyclopropenyl cation – the simplest Huckel's aromatic molecule – and its cyclic methyl derivatives in Titan's upper atmosphere. Planet. Space Sci. 87, 96.

Ali, A., Sittler Jr., E.C., Chornay, D., Rowe, B.R., Puzzarini, C., 2015. Organic chemistry in Titan's upper atmosphere and its astrobiological consequences: I. Views towards Cassini plasma spectrometer (CAPS) and ion neutral mass spectrometer (INMS) experiments in space. Planet. Space Sci. 109-110, 46–63.

Anders, E., Ebihara, M., 1982. Solar-system abundances of the elements. Geochim. Cosmochim. Acta 46, 2363–2380.

Artemieva, N., Lunine, J., 2003. Cratering on Titan: impact melt, ejecta, and the fate of surface organics. Icarus 164 (2003), 471–480. https://doi.org/10.1016/S0019-1035(03)00148-9.

Battistoni, G., Ferrari, A., Montaruli, T., Sala, P.R., 2003. The FLUKA atmospheric neutrino flux calculation. Astropart. Phys. 19, 269–290.

Becker, L., Poreda, R.J., Nuth, J.A., Ferguson, F.T., Liang, F., 2006. Fullerenes in meteorites and the nature of planetary atmospheres. In: Rietmeijer, Frans.J.M. (Ed.), Natural Fullerenes and Related Structures of Elemental Carbon. Springer, pp. 95–121.

Bernard-Salas, J., Cami, J., Peeters, E., Jones, A.P., Micelotta, E.R., Groenewegen, M.A.T., M.A.T., 2012. On the excitation and formation of circumstellar fullerenes. Astrophys. J. 757 (41). https://doi.org/10.1088/0004-637X/757/1/41. (11pp).

Borucki, W.J., Whitten, R.C., Bakes, E.L.O., Barth, E., Tripathi, S., 2006. Predictions of the electrical conductivity and charging of the aerosols in Titan's atmosphere. Icarus 181 (2), 527–544. https://doi.org/10.1016/j.icarus.2005.10.030.

Brun, R., Bruyant, F., Carminati, F., Giani, S., Maire, M., McPherson, A., et al., 1994. GEANT: Detector description and simulation tool. CERN Program Library Long Writeup W5013. CERN (Conseil Européen pour la Recherche Nucléaire), Geneva, Switzerland. https://doi.org/10.17181/CERN.MUHF.DMJ1. https://cds.cern.ch/record/1082634?ln=en.

Brünken, S., Gupta, H., Gottlieb, C.A., McCarthy, M.C., Thaddeus, P., 2007. Detection of the carbon chain negative ion C_8H^- in TMC-1. Astrophys. J. 664, L43–L46.

Burger, M.H., Sittler, E.C., Johnson, R.E., Smith, H.T., Tucker, O.J., Shematovich, V.I., 2007. Understanding the escape of water from Enceladus. J. Geophys. Res. 122. https://doi.org/10.1029/2006JA012,086.

Caldwell, K.A., Giblin, D.E., Gross, M.L., 1992. High energy collisions of fullerene radical cations with noble gases: capture of the target gas and charge stripping of C60+, C70+ and C84+. J. Am. Chem. Soc. 114, 3743–3756.

Cami, J., Bernard-Salas, J., Peeters, Els, Malek, S.E., 2010. Detection of C_{60} and C_{70} in a young planetary nebula. Science 329 (5996), 1180–1182.

Campbell, E.K., Holz, M., Gerlich, D., Maier, J.P., 2015. Laboratory confirmation of C_{60}^+ as the carrier of two diffuse interstellar bands. Nature 523, 322–328.

Crary, F.J., Magee, B.A., Mandt, K., Waite Jr, J.H., Westlake, J., Young, D.T., 2009. Heavy ons,temperatures and windsinTitan’s ionosphere: Combined Cassini CAPS and INMS observations. Planet. Space Sci. 57, 1847–1856. https://doi.org/10.1016/j.pss.2009.09.006.

Coates, A.J., Crary, F.J., Lewis, G.R., Young, D.T., Waite Jr., J.H., Sittler Jr., E.C., 2007. Geophys. Res. Lett. 34, L22103. https://doi.org/10.1029/2007GL030978.

Coates, A.J., Wellbrock, A., Lewis, G.R., Jones, G.H., Young, D.T., Crary, F.J., Waite Jr., J.H., 2009. Heavy negative ions in Titan's ionosphere: altitude and latitude dependence. Planet. Space Sci. 57 (14–15), 1866–1871. https://doi.org/10.1016/j.pss.2009.05.009.

Cooper, J.F., Sturner, S.J., 2018. Energetic radiation from galactic cosmic ray interactions with Saturn's main rings. J. Geophys. Res. Space Phys. 123. https://doi.org/10.1029/2018JA025583.

Cornet, T., Cordier, D., Bahers, T.L., Bourgeois, O., Fleurant, C., Mouélic, S.L., Altobelli, N., 2015. Dissolution on Titan and on earth: toward the age of Titan's karstic landscapes. J. Geophys. Res. Planets 120 (6), 1044–1074.

Cravens, T.E., Robertson, I.P., Ledvina, S.A., Michell, D., Krimigis, S.M., Waite Jr., J.H., 2008. Energetic ion precipitation at Titan. Geophys. Res. Let. 35, 03103. https://doi.org/10.1029/2007GL032451.

Desai, R.T., Coates, A.J., Wellbrock, A., Vuitton, V., Crary, F.J., González-Caniulef, D., Shebanits, O., Jones, G.H., Lewis, G.R., Waite, J.H., Cordiner, M., Taylor, S.A., Kataria, D.O., Wahlund, J.-E., Edberg, N.J.T., Sittler, E.C., 2017. Carbon chain anions and the growth of complex organic molecules in Titan's ionosphere. Astrophys. J. Lett. 844 (L18). https://doi.org/10.3847/2041-8213/aa7851. (6pp, 2017 August 1).

Ehrenfreund, P., Foing, B.H., 2010. Fullerene and cosmic carbon. Science 329, 1159–1160.

Ehrenfreund, P., Foing, B.H., 2015. Fullerene solves interstellar puzzle. Nature 523, 296.

Ehrenfreund, P., Glavin, D.P., Botta, O., Cooper, G., Bada, J.L., 2001. Extraterrestrial amino acids in Orgueil and Ivuna: tracing the parent body of CI type carbonaceous chondrites. PNAS 98 (5). www.pnas.orgycgiydoiy10.1073ypnas.051502898.

Elsila, J.E., Glavin, D.P., Dworkin, J.P., 2009. Cometary glycine detected in samples returned by stardust. Meteorit. Planet. Sci. 44, 1323–1330.

Engel, M.H., Nagy, B., 1982. Distribution and enantiomeric composition of amino acids in the Murchison meteorite. Nature 296, 837–840.

Foing, B.H., Ehrenfreund, P., 1994. Detection of two interstellar absorption bands coincident with spectral features of C_{60}^+. Nature 369, 296.

Foing, B.H., Ehrenfreund, P., 1997. New evidences for interstellar C_{60}^+. Astron. Astrophys. 317, L59.

Galazutdinov, G.A., Krelowski, J., Museav, F.A., Ehrenfreund, P., Foing, B.H., 2000. On the identification of the C_{60}^+ interstellar features. Mon. Not. R. Astron. Soc. 317, 750.

Garcia-Hernández, D.A., Diaz-Luis, J.J., 2013. Diffuse interstellar bands in fullerene planetary nebulae: the fullerenes – diffuse interstellar bands connection. Astron. Astrophys. 550 (L6, 5 pp.).

Hansen, C.J., Esposito, L., Stewart, A.I.F., Colwell, J., Hendrix, A., Pryor, W., Shemansky, D., West, R., 2006. Enceladus' water vapor plume. Science 311, 1422–1425.

Hartle, R.E., Sittler Jr., E.C., Neubauer, F.M., Johnson, R.E., Smith, H.T., Crary, F., et al., 2006a. Preliminary interpretation of titan plasma interaction as observed by the Cassini plasma spectrometer: comparisons with voyager 1. Geophys. Res. Lett. 33, L08201. https://doi.org/10.1029/2005GL024817.

Hartle, E.C., Sittler Jr., E.C., Neubauer, F.M., Johnson, R.E., Smith, H.T., Crary, F., et al., 2006b. Initial interpretation of titan plasma interaction as observed by the Cassini plasma spectrometer: comparisons with voyager 1. Planet. Space Sci. 54, 1211.

Hayes, A., Aharonson, O., Callahan, P., Elachi, C., Gim, Y., Kirk, Y.R., Lewis, K., et al., 2008. Hydrocarbon lakes on Titan: distribution and interaction with a porous regolith. Geophys. Res. Lett. 35, L09204. https://doi.org/10.1029/2008GL033409.

Herbst, E., 1981. Can negative molecular ions be detected in dense interstellar clouds? Nature 289, 656.

Herbst, E., Osamura, Y., 2008. Calculations on the formation rates and mechanisms for C_nH anions in interstellar and circumstellar media. Astrophys. J. 679, 1670–1679.

Heyman, D., 1986. Buckminsterfullerenes its siblings and soot: Carriers of trapped inert gases in meteorites? J. Geophys. Res. 91, E135–E138.

Hörst, S.M., Tolbert, M.A., 2013. In situ measurements of the size and density of Titan aerosol analogs. Astrophys. J. Lett. 770, L10. (6pp). https://doi.org/10.1088/2041-8205/770/1/L10.

Hörst, S.M., Vuitton, V., Yelle, R.V., 2008. The origin of oxygen species in Titan's atmosphere. J. Geophys. Res. 113, E10006. https://doi.org/10.1029/2008JE003135.

Hudson, R.L., Moore, M.H., Dworkin, J.P., Martin, M.P., Pozun, Z.D., 2008. Amino acids from ion-irradiated nitrile-containing ices. Astrobiology 8 (4). https://doi.org/10.1089/ast.2007.0131. 2008, © Mary Ann Liebert, Inc.

Jaumann, R., Kirk, R.L., Lorenz, R.D., Lopes, R.M.C., Stofan, E., Turtle, E.P., et al., 2009a. Geology and surface processes on Titan. In: Brown, R.H. (Ed.), Titan From Cassini-Huygens. Springer, pp. 75–140.

Jaumann, R., Clark, R.N., Nimmo, F., Hendrix, A.R., Buratti, B.J., Denk, T., Moore, J.M., Schenk, P.M., Ostro, S.J., Srama, R., 2009b. Icy satellites: geological evolution and surface properties. In: Dougherty, M.K. (Ed.), Saturn From Cassini-Huygens. 637–681 Springer.

Johnson, R.E., Liu, M., Sittler Jr., E.C., 2005. Plasma-induced clearing and redistribution of material embedded in planetary magnetospheres. Geophys. Res. Lett. 32, L24201. https://doi.org/10.1029/2005GL024275.

Johnson, R.E., Luhmann, J.G., Tokar, R.L., Bouhram, M., Berthelier, J.J., Sittler, E.C., et al., 2006a. Production, ionization and redistribution of O_2 in Saturn's ring atmosphere. Icarus 180 (2), 393–402.

Johnson, R.E., Smith, H.T., Tucker, O.J., Liu, M., Burger, M.H., Sittler Jr., E.C., Tokar, R.L., 2006b. The Enceladus and OH Tori at Saturn. Astrophys. J. 644, L137–L139.

Kaiser, A., Zöttl, S., Bartl, P., Leidlmair, C., Mauracher, A., Probst, M., Denifl, S., Echt, O., Scheier, P., 2013. Methane adsorption on aggregates of fullerenes: site-selective storage capacities and adsorption energies. ChemSusChem 6, 1235–1244. https://doi.org/10.1002/cssc.201300133.

Khare, B., Sagan, C., Thompson, W.R., Arakawa, E.T., Meisse, C., Tuminello, P.S., 1994. Can. J. Chem. 72, 678.

Krasnopolsky, A., 2012. Titan's photochemical model: further update, oxygen species, and comparison with Triton and Pluto. Planet. Sp. Sci. 73, 318–326.

Krätschmer, W., Lamb, L.D., Fostiropoulos, K., Huffman, D.R., 1990. Solid C_{60}: a new form of carbon. Nature 347, 354–358.

Kroto, H.W., McKay, K., 1988. The formation of quasi-icosahedral spiral shell carbon particles. Nature 331, 328.

Kroto, H.W., Heath, J.R., O'Brien, S.C., Curl, R.F., Smalley, R.E., 1985. C_{60}: Buckminsterfullerene. Nature 318, 162–163.

Kroto, H.W., Allaf, A.W., Balm, S.P., 1991. C_{60}: Buckminsterfullerene. Chem. Rev. 91, 1213–1235.

Kuan, Yi-Jehng, Charnley, S.B., Huang, Hui-Chun, Tsong, Wei-Ling, Kisiel, Z., 2003. Interstellar glycine. Astrophys. J. 593, 848–867.

Kvenvolden, K.A., et al., 1970. Evidence for extraterrestrial amino acids and hydrocarbons in the Murchison meteorite. Nature 228 (5275), 923–926. https://doi.org/10.1038/228923a0.

Lavvas, P., Yelle, R.V., Koskinen, T., Bazinc, A., Vuitton, V., Vigrend, E., et al., 2013. Aerosol growth in Titan's ionosphere, Proc. Nat. Acad. Sci. 110 (8), 2729–2734.

Lewis, R.S., Srinivasan, B., Anders, E., 1975. eHost phase of a Strange Xenon component in Allende. Science 190 (4221), 1251–1262.

Liang, M.-C., Yung, Y.L., Shemansky, D.E., 2007. Photolytically generated aerosols in the mesosphere and thermosphere of Titan. Astrophys. J. Lett. 661, L199–L202.

Lopes, R.M.C., Kirk, R.L., Mitchell, K.L., LeGall, A., Barnes, J.W., Hayes, A., Kargel, J., Wye, L., Radebaugh, J., Stofan, E.R., Janssen, M.A., Neish, C.D., Wall, S.D., Wood, C.A., Lunine, J.I., Malaska, M.J., 2013. Cryovolcanism on Titan: New results from Cassini RADAR and VIMS. J. Geophys. Res. Planets. https://doi.org/10.1002/jgre.20062. (12 February).

Lorenz, R.D., 2014. Physics of saltation and sand transport on Titan: A brief review. Icarus 230 (2014), 162–167.

Lorenz, R.D., Kraal, E., Asphaug, E., Thomson, R.E., 2003. EOS Trans. 84, 125.

Lorenz, R.D., Wood, C.A., Lunine, J.I., Wall, S.D., Lopes, R.M., Mitchell, K.L., Paganelli, F., Anderson, Y.Z., Wye, L., Tsai, C., Zebker, H., Stofan, E.R., 2007. Titan's young surface: Initial impact crater survey by Cassini RADAR and model comparison. Geophys. Res. Lett. 34 (7). https://doi.org/10.1029/2006GL028971.

Lunine, J.I., 1990. Evolution of the atmosphere and surface of Titan. ESA SP-315, 159–165.

Martin, T.P., et al., 1996. Clusters of fullerenes molecules and metal atoms, Physica. Scripta. T66, 38–47.

Mastrogiuseppe, M., Poggiali, V., Hayes, A., Lorenz, R., Lunine, J., Picardi, G., et al.,

2014. The bathymetry of a Titan sea. Geophys. Res. Lett. 41, 1432–1437. https://doi.org/10.1002/2013GL058618.

Matthiä, D., Hassler, D.M., de Wet, W., Ehresmann, B., Firan, A., Flores-McLaughlin, J., Guo, J., Heilbronn, L.H, Lee, K., Ratliff, H., 2017. The radiation environment on the surface of Mars - summary of model calculations and comparison to RAD data. Life Sci. Space Res. 14, 18–28.

McCarthy, M.C., Gottlieb, C.A., Gupta, H., Thaddeus, P., 2006. Laboratory and astronomical identification of the negative molecular ion C_6H^-. Astrophys. J. 652, L141–L144.

Molina-Cuberos, G.J., López-Moreno, J.J., Rodrigo, R., Lara, L.M., O'Brien, K., 1999. Ionization by cosmic rays of the atmosphere of Titan. Planet. Space Sci. 47, 1347–1354.

Morales, S.B., Le Picard, S.D., Canosa, A., Sims, I.R., 2010. Experimental measurements of low temperature rate coefficients for neutral-neutral reactions of interest for atmospheric chemistry of Titan, Pluto and Triton: reactions of the CN radical, Chemistry of the Planets, Faraday **147** Conference. pp. 155 (Brittany France).

Neish, C.D., Lorenz, R.D., 2012. Titan's global crater population: a new assessment. Planet. Space Sci. 60, 26–33. https://doi.org/10.1016/j.pss.2011.02.016.

Neish, C.D., Molaro, J.L., Lora, J.M., Howard, A.D., Kirk, R.L., Schenk, P., Bray, V.J., Lorenz, R.D., 2016. Fluvial erosion as a mechanism for crater modification on Titan. Icarus 270, 114–129. https://doi.org/10.1016/j.icarus.2015.07.022.

Niemann, H.B., Atreya, S.K., Bauer, S.J., Carignan, G.R., Demick, J.E., Frost, R.L., Gautier, D., Haberman, J.A., Harpold, D.N., Hunten, D.M., Israel, G., Lunine, J.I., Kasprzak, W.T., Owen, T.C., Paulkovich, M., Raulin, F., Raaen, E., Way, S.H., 2005. The composition of Titan's atmosphere from the GCMS on the Huygen probe, and implications for the origin of nitrogen and methane. Nature 438, 779–784. https://doi.org/10.1038/nature04122.

Niemann, H.B., Atreya, S.K., Demick, J.E., Gautier, D., Haberman, J.A., Harpold, D.N., Kasprzak, W.T., Lunine, J.I., Owen, T.C., Raulin, F., 2010. Composition of Titan's lower atmosphere and simple surface volatiles as measured by the Cassini-Huygens probe gas chromatograph mass spectrometer experiment. J. Geophys. Res. 115, E12006. https://doi.org/10.1029/2010JE003659.

Oro, J., Gibert, J., Lichtenstein, H., Wikstrom, S., Flory, D.A., March 12, 1971. Amino-acids, aliphatic and aromatic hydrocarbons in the Murchison meteorite. Nature 230, 105–106.

Otsuka, M., et al., 2013. The detection of C_{60} in the well-characterized planetary nebula M1-11. Astrophys. J. 764 (77), 20. https://doi.org/10.1088/0004-637X/764/1/77.

Pietzak, B., et al., 1997. Buckminsterfullerene C60: a chemical Faraday cage for atomic nitrogen. Chem. Phys. Lett. 21, 259–263.

Porco, C.C., et al., 2005. Imaging of Titan from the Cassini spacecraft. Nature 434, 159–168.

Porco, C.C., Helfenstein, P., Ingersoll, P.C., Wisdom, J., West, R., Neukum, G., et al., 2006. Cassini observes the active south pole of Enceladus. Science 311, 1393–1401.

Potgieter, M.S., Vos, E.E., Munini, R., Boezio, M., Di Felice, V., 2015. Modulation of Galactic Electrons in the Heliosphere during the Unusual Solar Minimum of 2006–2009: A Modeling Approach. Astrophys. J. 810 (2) id. 141, 10 pp. https://doi.org/10.1088/0004-637X/810/2/141.

Raulin, F., Owen, T., 2002. Organic chemistry and exobiology on Titan. Space Sci. Rev. 104 (1–2), 379.

Remijan, A.J., et al., 2007. Detection of C_8H^- and comparison with C_8H toward IRC + 10 216. Astrophys. J. 664, L47–L50.

Robertson, I.P., Cravens, T.E., Waite Jr., J.H., Yelle, R.V., Vuitton, V., Coates, A.J., Wahlund, J.E., Ågren, K., Mandt, K., Magee, B., Richard, M.S., Fattig, E., 2009. Structure of Titan's ionosphere: model comparisons with Cassini data. Planet. Space Sci. 57, 2008 1834–1846.

Sagan, C., Thompson, W.R., Khare, B.N., 1992. Titan: a laboratory for prebiological organic chemistry. Acc. Chem. Res. 1992 (25), 286–292.

Sakai, N., Sakai, T., Yamamoto, S., 2007. Detection of C_6H^- toward the low-mass protostar IRAS 04368 + 2557 in L1527. Astrophys. J. 667, L65–L68.

Sakai, N., et al., 2008. Tentative detection of C_4H^- toward the low-mass protostar IRAS 04368 + 2557 IN l1527. Astrophys. J. 673, L71–L74.

Sellgren, K., Werner, M.W., Ingalls, J.G., Smith, J.D.T., Carleton, T.M., Joblin, C., 2010. C60 in reflection nebulae. Astrophys. J. Lett. 722, L54–L57.

Sittler Jr., E.C., 2010. Faraday Discuss. Chemistry of the Planets, Faraday 147 Conference 147, 379–403 Brittany France, 155.

Sittler Jr., E.C., Andre, N., Blanc, M., Burger, M., Johnson, R.E., Coates, A.J., et al., 2008. Ion and neutral sources and sinks within Saturn's inner magnetosphere: Cassini results. Planet. Space Sci. 56, 3–18.

Sittler Jr., E.C., Ali, A., Cooper, J.F., Hartle, R.E., Johnson, R.E., Coates, A.J., Young, D.T., 2009a. Heavy ion formation in Titan's ionosphere: magnetospheric introduction of free oxygen and a source of Titan's aerosols? Planet. Space Sci. 57, 1547–1557. https://doi.org/10.1016/j.pss.2009.07.017.

Sittler Jr., E.C., Hartle, R.E., Bertucci, C., Coates, A.J., Cravens, T., Dandouras, I., Shemansky, D., 2009b. Energy Deposition Processes in Titan's Upper Atmosphere and its Induced Magnetosphere. In: Brown, R.H., Lebreton, Jean-Pierre, Waite, J.H. (Eds.), Titan from Cassini-Huygens. Springer, pp. 393–454.

Stofan, E.R., et al., 2007. The lakes of Titan. Nature 445 (7123), 61–64. https://doi.org/10.1038/nature05438.

Sturner, S.J., Seifert, H., Shrader, C.R., Teegarden, B.J., 2000. MGEANT - A GEANT-based multi-purpose simulation package for gamma-ray astronomy missions. In: McConnell, M.L., Ryan, J.M. (Eds.), Proceedings of the Fifth Compton Symposium (p. 814). American Institute of Physics, New York.

Snyder, L.E., Lovas, F.J., Hollis, J.M., Friedel, D.N., Jewell, P.R., Remijan, A., Ilyushin, V.V., Alekseev, E.A., Dyubko, S.F., 2005. A Rigorous attempt to verify interstellar glycine. Astrophys. J. 619, 914–930 (February 1).

Thaddeus, P., 1994. On the large organic molecules in the interstellar gas. In: Nenner, Iréne (Ed.), Molecules and Grains in Space, AIP Conference Proceedings 312. 1993. Mont Sainte-Odile, France, pp. 711–731.

Thaddeus, P., 1995. Carbon chains and the diffuse interstellar bands. In: Tielens, A.G.G.M., Snow, T.P. (Eds.), The Diffuse Interstellar Bands. Kluwer Academic Publishers, The Netherlands, pp. 369–378.

Thaddeus, P., Gottlieb, C.A., Gupta, H., Brünken, S., McCarthy, M.C., Agúndez, M., et al., 2008. Laboratory and astronomical detection of the negative molecular ion C_3N^-. Astrophys. J. 677, 1132–1139.

Thompson, W.R., Sagan, C., 1992. Organic chemistry on Titan. Surface interactions. In: Proc. of the Symposium on Titan. In: ESA SP. 338. ESA, Noordwijk, pp. 167–176.

Vuitton, V., Lavvas, P., Yelle, R.V., Galand, M., Wellbrock, A., Lewis, G.R., et al., 2009. Negative ion chemistry in Titan's upper atmosphere. Planet. Space Sci. 57, 1558–1572.

Waite, J.H., et al., 2009a. Liquid water on Enceladus from observations of ammonia and ^{40}Ar in the plume. Nature 460, 487–490.

Waite, J.H., et al., 2009b. High-Altitude production of Titan's aerosols. In: Brown, R.H., Lebreton, J.-P., Waite, J.H. (Eds.), Titan from Cassini-Huygens. Springer, pp. 201–214.

Waite Jr., J.H., et al., 2007. The process of tholin formation in Titan's upper atmosphere. Science 316, 870. https://doi.org/10.1126/science.1139727.

Wang, X.-B., Wang, L.-S., 2009. Annual reviews of. Physical Chemistry 60, 105.

Weidinger, A., et al., 1998. Atomic nitrogen in C60:N@C60. Appl. Phys. A 66, 287–292.

Weiske, T., et al., 1991. Injection of helium atoms into doubly and triply charged C60 cations. J. Phys. Chem. 95, 8451–8452.

Wood, C.A., Lorenz, R., Kirk, R., Lopes, R., Mitchell, K., Stofan, E., The Cassini RADAR Team, 2010. Impact craters on Titan, Icarus 206 (2010), 334–344.

Yelle, R.V., Strobell, D.F., Lellouch, E., Gautier, D., 1997. Engineering Models for Titan's Atmosphere, In Huygens: Science, Payload and Mission. In: Wilson, A. (Ed.), Proceedings of an ESA conference, pp. 243–256.

Yelle, R.V., Vuitton, V., Lavvas, P., Klippenstein, S.J., Smith, M.A., Hörst, S.M., Cui, J., 2010. Formation of NH3 and CH2NH in Titan's upper atmosphere. Faraday Discuss. 147, 31–49. https://doi.org/10.1039/c004787m.

Zarnecki, J.C., Leese, M.R., Hathi, B., Ball, A.J., Hagermann, A., Towner, M.C., Lorenz, R.D., McDonnell, J.A.M., Green, S.F., Patel, M.R., Ringrose, T.J., Rosenberg, P.D., Atkinson, K.R., Paton, M.D., Banaszkiewicz, M., Clark, B.C., Ferri, F., Fulchignoni, M., Ghafoor, N.A.L., Kargl, G., Svedhem, H., Delderfield, J., Grande, M., Parker, D.J., Challenor, P.G., Geake, J.E., 2005. A soft solid surface on Titan as revealed by the Huygens Surface Science Package. Nature 438, 792–795. https://doi.org/10.1038/nature04211.

Zeitnitz, C., Gabriel, T.A., 1994. The GEANT-CALOR interface and benchmark calculations of ZEUS test calorimeters. Nucl. Instrum. Meth. Phys. Res. A 349 (1994), 106–111.

Zhang, Q.L., O'Brien, S.C., Heath, J.R., Liu, Y., Curl, R.F., Kroto, H.W., Smalley, R.E., 1986. Reactivity of Large Carbon Clusters: Spheroidal Carbon Shells and Their Possible Relevance to the Formation and Morphology of Soot. J. Phys. Chem. 90 (4) February 13, 1986).